European Journal of Medicinal Chemistry 164 (2019) 440–447

Contents lists available at ScienceDirect

European Journal of Medicinal Chemistry

journal homepage: http://www.elsevier.com/locate/ejmech

Research paper

Discovery of novel anti-angiogenesis agents. Part 9: Multiplex inhibitors suppressing compensatory activations of RTKs

Yuanyuan Shan [a], Ru Si [c], Jin Wang [c], Qingqing Zhang [c], Huaxin Zhou [c], Jie Song [c], Jie Zhang [c, *], Qinhua Chen [b, **]

[a] Department of Pharmacy, The First Affiliated Hospital of Xi'an Jiaotong University, Xi'an, 710061, China
[b] Affiliated Dongfeng Hospital, Hubei University of Medicine, Shiyan, 442008, China
[c] School of Pharmacy, Health Science Center, Xi'an Jiaotong University, Xi'an, 710061, China

ARTICLE INFO

Article history:
Received 11 September 2018
Received in revised form
25 December 2018
Accepted 25 December 2018
Available online 28 December 2018

Keywords:
Anti-angiogenic agents
Multi-target
RTK inhibitors
Compensatory activation
1,2,3-Triazole

ABSTRACT

Aberrant angiogenesis is a hallmark of various diseases including cancers. VEGFR-2 inhibitors have been utilized as anti-angiogenic agents for several years. However, compensatory activation of various receptor tyrosine kinases (RTK) could induce the occurrence of resistance. We previously reported a series of multi-target inhibitors of VEGFR-2, Tie-2, and EphB4 as anti-angiogenic agents. These inhibitors might be a promising strategy to overcome the resistance induced by compensatory activation. In order to expand the structural diversity of these multiple RTK inhibitors, we described herein the design, synthesis, and evaluation of a novel class of triplet VEGFR-2/TIE-2/EphB4 inhibitors. The biological evaluation indicated that five compounds (**6b, 6d, 6e, 7e**, and **7g**) exhibited simultaneous VEGFR-2/Tie-2/EphB4 inhibitory activities with IC_{50} values less than 50 nM.

© 2018 Elsevier Masson SAS. All rights reserved.

1. Introduction

Angiogenesis is a complex multifactorial process involving multiple angiogenic factors, including pro-angiogenic factors and anti-angiogenic factors. Pathological angiogenesis is usually accompanied by excessive activation of multiple pro-angiogenic factors [1]. Among these pro-angiogenic factors, vascular endothelial growth factor (VEGF) and its receptor (VEGFR) are the most important pro-angiogenic factors. It could increase vascular permeability and promote proliferation, migration and survival of vascular endothelial cells [2]. Angiopoietin (Ang) and its receptor (Tie-2) could inhibit endothelial cell apoptosis, and promote vascular bud, branch, reshape and mature [3]. Erythropoietin producing hepatocyte receptor B4 (EphB4) and its membrane adherent ligand (EphrinB2) are essential for angiogenesis, vascular maturation, and pericytes recruitment [4]. All of them mentioned above belong to the receptor tyrosine kinase family (RTK), which plays an important role in signal transduction and is an indispensable regulator of angiogenesis [5].

The mechanism of resistance of anti-angiogenic agents is highly variable. Extensive investigations linked drug resistance with compensatory activation of angiogenic receptor tyrosine kinases (RTKs) [6]. The compensatory activation of pro-angiogenic factors such as VEGFR-2, Tie-2 and EphB4 is the main mechanisms that may lead to poor responsiveness and resistance [7]. Accordingly, we propose that multiplex inhibition of VEGFR-2, EphB4, and Tie-2 might enhance anti-angiogenesis effect and overcome the resistance [8]. Meanwhile, it is feasible to develop multiplex inhibitors of VEGFR-2/Tie-2/EphB4 because of their highly conserved ATP-binding pocket. The catalytic domains and ATP-binding site in the active conformation of these RTKs are notably similar [9–12]. Moreover, it is reasonable to assume that all the ATP-competitive RTK inhibitors bind to the ATP pocket [13].

We previously reported a series of thioureas as multiple RTK inhibitors which displayed considerable potential as anti-angiogenic and anticancer agents [14]. Inspiringly, DATU1 exhibited simultaneous inhibitory activities against EphB4 and Tie-2. In the current research, our continuous efforts focused on the development of novel multi-target RTK inhibitors as anti-angiogenic agents. These inhibitors share a basic architecture for construction which can be divided into four segments. Segment A could

* Corresponding author.
** Corresponding author.
E-mail addresses: zhj8623@mail.xjtu.edu.cn (J. Zhang), cqh77@163.com (Q. Chen).

https://doi.org/10.1016/j.ejmech.2018.12.067
0223-5234/© 2018 Elsevier Masson SAS. All rights reserved.

form hydrogen bonds with hinge of RTK, while segment C form hydrogen bonds with the conserved Glu and DFG-motif of RTK. These two segments are essential for interaction with receptors. Therefore, we explored the structural diversity of segment A and segment C with DATU1 as novel lead compound (Fig. 1). Aromatic-heterocyclics such as pyridine, pyrimidine, and pyrazole were incorporated as hinge binding group. We reasoned that it is possible that these groups could form hydrogen bonds with hinge region of RTKs. It is well known that the presence of electron-attractors such as chlorine and fluorine in a molecule could enhance drug persistence and lipid solubility. Therefore, aniline which contained one or more halogen substituents were incorporated as electron-attractors as they were beneficial for anticancer potency and could enhance the persistence. Moreover, thiourea in DATU1 was replaced with triazole to expand the structural diversity and improve the activity of these multiple RTK inhibitors.

With these results in hand, we proposed that simultaneous inhibition of RTKs could afford novel anti-angiogenic agents. Finally, 20 title compounds (8 pyrimidines and 12 pyrazoles) were prepared through acylation, Suzuki coupling and click reaction. All of these compounds were confirmed by MS and NMR. Biological evaluations including inhibition against VEGFR-2/Tie-2/EphB4 and anti-proliferative activity against human umbilical vein endothelial cell (EA.hy926) were carried out. Biological evaluation indicated that several title compounds displayed simultaneous inhibition against three pro-angiogenic RTKs. Meanwhile, some of them also exhibited potent anti-proliferative potency against human vascular endothelial cell (EA.hy926). Subsequently, molecular docking was performed to rationalize the efficiency of the potent compound with multiplex inhibition profile.

2. Results and discussion

2.1. Chemistry

The synthesis procedure of the title compounds **6a-6h** was outlined in Scheme 1. Commercially available 1-bromo-4-(bromomethyl)benzene reacted with NaN_3 to afford 1-(azidomethyl)-4-bromobenzene **3** [15]. Copper-catalyzed azide-alkyne cycloaddition reaction (click reaction) between azide **3** and various phenylacetylene **1** was used to afford the key intermediate, 1,2,3-triazoles **4** [16]. Palladium catalyzed coupling of 1,2,3-triazoles **4** with pyrimidin-5-ylboronic acid **5** in the presence of cesium carbonate in a mixture of water/dioxane under refluxing conditions overnight afforded title compounds **6a-6g** [17]. Acylation of **6g** with cyclopropanecarbonyl chloride yield the title compound **6h** [18].

Title compounds **7a-7l** were prepared using the synthetic route described in Scheme 1. Firstly, 1-(azidomethyl)-4-bromobenzene **3** was prepared from commercially available 1-bromo-4-(bromomethyl)benzene **2**. Subsequently, the synthesis of the key intermediates 1,2,3-triazoles **4** was performed via cycloaddition between azide **3** and various phenylacetylene **1** [19]. $Pd(PPh_3)_4$ catalyzed Suzuki coupling of 1,2,3-triazoles **4** with 4-(4,4,5,5-tetramethyl-1,3,2-dioxaborolan-2-yl)-1H-pyrazole **5** in presence of cesium carbonate in a mixture of water/dioxane under refluxing conditions afforded the title compounds **7a-7k** [20]. Finally, the title compounds **7l** were prepared through acylation of **7k** with cyclopropanecarbonyl chloride. All the title compounds are characterized by ^{1}H-NMR, ^{13}C-NMR, and melting point analysis (Supplementary Material).

2.2. Biology assays

In order to evaluate the biological activities of title compounds as anti-angiogenic agents, we firstly tested the enzymatic inhibitory activity of the title compounds against three angiogenic RTKs, VEGFR-2, Tie-2, and EphB4. Subsequently, their inhibition on viability of HUVECs (EA.hy926) was evaluated to prove the anti-angiogenic potency. In parallel, a marketed multi-target RTK inhibitors, Sorafenib, was used as positive control.

2.2.1. Angiogenic receptor tyrosine kinases inhibition assay

The inhibitory activities of title compounds on VEGFR-2, Tie-2, and EphB4 kinase were evaluated using ADP-Glo Kinase Assay Kit (Promega, Wisconsin, USA) [21]. The biological evaluation results were depicted in Table 1 and Table 2 with Sorafenib as the positive control.

In analyzing the biological results, we first look at the implications of hinge binding group by replacement of pyridine with pyrimidine and pyrazole. The results indicated that five compounds (**6b, 6d, 6e, 7e**, and **7g**) displayed simultaneously inhibitory potency against VEGFR-2, Tie-2, and EphB4 with IC_{50} values less than 50 nM (Table 1). In particular, **7e** exhibited the most potent inhibitory activity against pro-angiogenic RTKs with IC_{50} values of 3.17 nM (VEGFR-2), 2.69 nM (Tie-2), and 0.16 nM (EphB4), respectively. The results suggested an important and favorable role of the *para*-fluoro and methyl substituents in the inhibition of VEGFR-2, Tie-2, and EphB4. There are five other title compounds (**6c, 7a, 7b, 7i**, and **7j**) were potent inhibitors against two pro-angiogenic RTKs with IC_{50} values less than 100 nM. They might be effective dual-target RTK inhibitors. The results highlighted the importance of *N*-methylpyrazole for improving the simultaneous inhibition of these multiple inhibitors. It has been verified that compounds bearing *N*-methylpyrazole were more potent than pyrazole and pyrimidine. This study identified that *N*-methylpyrazole could serve as an excellent hinge binding group for multi-target

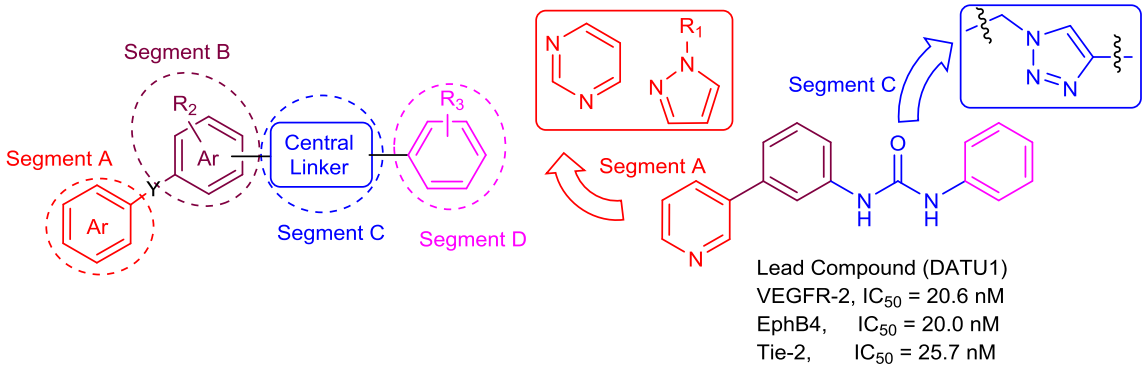

Fig. 1. The pharmacophore model of multi-target RTK inhibitors and structural optimization of lead compound (DATU1).

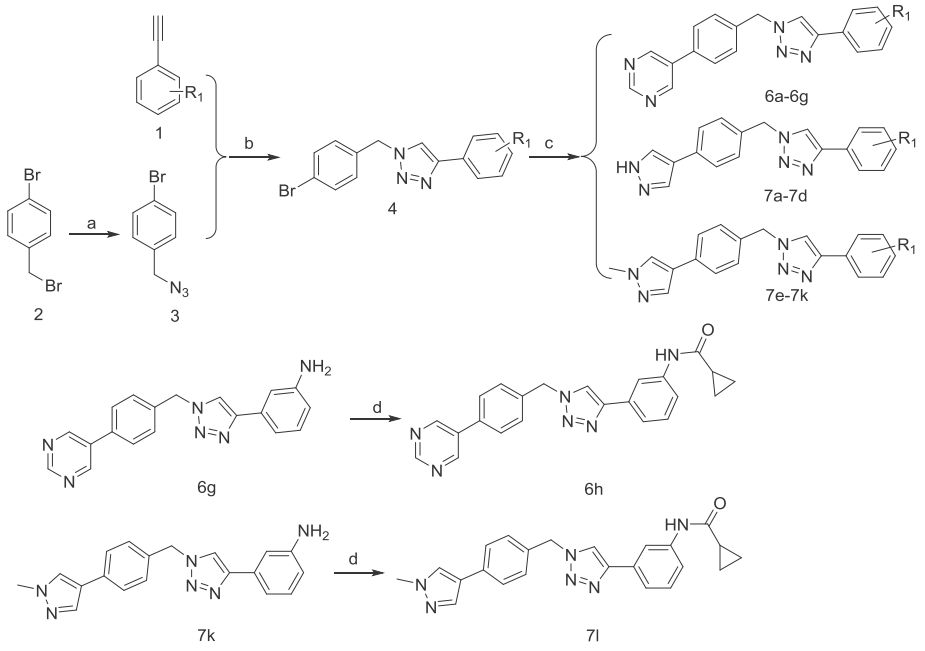

Scheme 1. Synthesis of title compounds (6a-6h) and (7a-7l). **Reagents and conditions**: (a) NaN_3, DMF, r.t., 12h; (b) *L*-Sodium ascorbate, copper sulfate pentahydrate, etanol, H_2O, r.t.; (c) pyrimidin-5-ylboronic acid (**5**), 4-(4,4,5,5-tetramethyl-1,3,2-dioxaborolan-2-yl)-1*H*-pyrazole (**5a**), or 1-methyl-4-(4,4,5,5-tetramethyl-1,3,2-dioxaborolan-2-yl)-1*H*-pyrazole (**5b**), pd(pddf)Cl_2, dioxane/H_2O, CS_2CO_3, reflux; (d) cyclopropyl carbonyl chloride, triethylamine, CH_2Cl_2, 0°C-r.t., 30min.

Table 1
Structures and RTKs inhibitory activities of title compounds (IC_{50}, nM)..

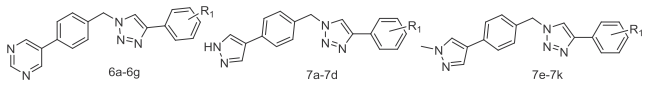

Compound	R_1	VEGFR-2	Tie-2	EphB4
6a	*meta*-Cl	ND	ND	>1000
6b	*ortho*-F	7.63	5.45	0.25
6c	H	>1000	51.86	0.32
6d	*para*-CH_3	11.06	25.74	3.30
6e	*meta*-CH_3	2.57	13.71	28.62
6f	*para*-CF_3	ND	>1000	>1000
6g	*meta*-NH_2	55.95	210	>1000
6h	*meta*-	125.06	>1000	>1000
7a	*para*-F	ND	5.46	73.15
7b	*meta*-CH_3	0.53	46.39	>1000
7c	*para*-CF_3	>1000	>1000	16.00
7d	*meta*-NH_2	>1000	>1000	>1000
7e	*para*-F	3.17	2.69	0.16
7f	H	500.28	>1000	1.49
7g	para-CH_3	0.57	77.42	2.13
7h	*meta*-CH_3	>1000	51.44	ND
7i	para-CF_3	>1000	9.11	2.21
7j	*meta*-CF_3	58.10	1.79	ND
7k	*meta*-NH_2	ND	>1000	>1000
7l	*meta*-	4.15	0.82	>1000
Sorafenib		0.17	0.39	0.22

inhibitors of VEGFR-2, Tie-2, and EphB4.

We are enlightened by the above potent multiple inhibitors with new hinge binding group. Subsequently, novel derivatives incorporated with *N*-methylpyrazole will be further developed as anti-angiogenic agents.

Table 2
Inhibition of compounds on human vascular endothelial cell viability (IC_{50}, μM).

Compound	EA.hy 926	Compound	EA. hy926	Compound	EA. hy926
6a	7.83	6h	17.26	7g	38.10
6b	22.54	7a	19.95	7h	1.11
6c	35.53	7b	134.15	7i	ND
6d	1.01	7c	20.93	7j	69.02
6e	142.28	7d	250.58	7k	22.01
6f	46.84	7e	1.90	7l	483.54
6g	30.21	7f	62.22	Sorafenib	11.74

2.2.2. Effects of title compounds on the human umbilical vein endothelial cells (EA.hy926) and cancer cells viability

With the aim of determining the potential anti-angiogenic effect of these multi-target inhibitors, we evaluate the anti-proliferative activity of title compounds on HUVECs (EA.hy926) using cell counting kit-8 (CCK-8) method [22]. Highly consistent with their potent RTK inhibitory activity, the majority of title compounds displayed dose-dependent inhibition of EA.hy926 viability with IC_{50} values ranging from 1.01 μM to 100 μM (Table 2). In particular, three compounds (**6d, 7e**, and **7h**) displayed more potent inhibition on viability of HUVECs than others with IC_{50} values less than 2.0 μM. These results demonstrated that these compounds might display anti-angiogenic potency through decreasing viability of HUVECs (EA.hy926).

RTKs play essential roles in the proliferation of various cancer cells and RTKs inhibition generally translate well into anti-proliferation activity. Therefore, in order to evaluate the anti-cancer activity, the most potent multiple RTK inhibitor, **7e**, was selected to test its anti-proliferative activity against several cancer cells including human breast cancer cell (MCF-7), human lung cancer cell (A549), human epidermoid carcinoma cell (A431), human cervical cancer cell (HeLa), and human colon carcinoma cell (LOVO). Compound **7e** was found to strongly inhibit the growth of all the five cancer cell lines with IC_{50} values ranging from 1.2 μM to 27.8 μM (Table 3). It exhibited comparable anti-proliferative

Table 3
Anti-proliferative activities of compound 7e against various cancer cells.

Compound	Cancer Cell Lines, IC_{50} (μM)				
	MCF-7	A549	A431	HeLa	LOVO
7e	15.55	1.20	7.29	27.80	1.32
Sorafenib	3.47	3.88	3.32	8.74	2.52

potency with Sorafenib. It displayed superior anti-proliferative potency to Sorafenib against human lung cancer cell (A549) and human colon carcinoma cell (LOVO) with IC_{50} values of 1.20 μM and 1.32 μM. In summary, 7e showed significant anti-proliferative activity against a broad spectrum of cancer cell lines.

2.2.3. Molecular docking study

For further structural optimization and investigation of the potential binding mode, molecular modeling studies were performed using Sybyl-X (Version 2.0, Tripos Inc. St. Louis, MO) [23]. The most potent compound, **7e**, was constructed and optimized using Powell's method with a Tripos force field. The molecular modeling was performed using Sybyl-X/Surflex-dock module, and the residues in a 5.0 Å radius around the natural ligand of VEGFR-2 (PDB ID: 4ASD), Tie-2 (PDB ID: 4X3J) and EphB4 (PDB ID: 4BB4) were selected as the active site. The binding mode of **7e** with the ATP-pocket of VEGFR-2, Tie-2, and EphB4 were described in Figs. 2–4. Favorable binding interactions of 7e with the active site of VEGFR-2 included two hydrogen bonds (Fig. 2): nitrogen atom in pyrazole of **7e** formed one hydrogen bond with Asn 923 in the hinge region of VEGFR-2 with distance of 2.30 Å. In addition, fluorine atom in terminal benzene formed one hydrogen bond with conserved Asp 1046 of DFG-motif with distance of 2.63 Å. As for Tie-2, the binding model was depicted in Fig. 3. Nitrogen atom of 1,2,3-triazole formed two hydrogen bonds with conserved Asp 982 with the distance of 2.36 Å and 2.59 Å, respectively. As shown in Fig. 4, fluorine atom in terminal benzene formed one hydrogen bond with conserved Met 696 with distance of 2.48 Å. Meanwhile, nitrogen atom of 1,2,3-triazole formed two hydrogen bonds with Thr 693 with the distance of 2.36 Å and 2.27 Å, respectively. These molecular docking results indicated that the 1,2,3-triazole moiety is beneficial for affinity of inhibitors with VEGFR-2, Tie-2, and EphB4. Our docking result may explain why compound **7e** shows activities on all three proteins. It could be considered as novel scaffold for further discovery of triple RTK inhibitors.

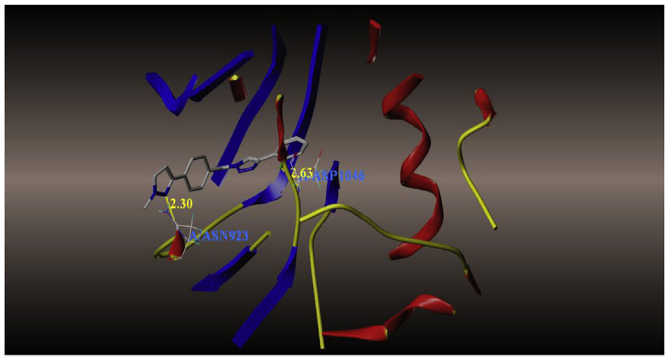

Fig. 2. Superimposition of the docking poses for VEGFR-2 (PDB ID: 4ASD) with compound (7e) and native ligand (cyan). Hydrogen bonds were depicted in dashed yellow lines. (For interpretation of the references to colour in this figure legend, the reader is referred to the Web version of this article.)

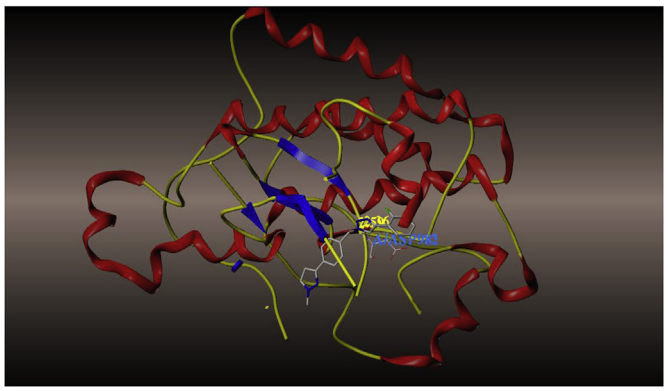

Fig. 3. Superimposition of the docking poses for Tie-2 (PDB ID: 4X3J) with compound (7e) and native ligand (cyan). Hydrogen bonds were depicted in dashed yellow lines. (For interpretation of the references to colour in this figure legend, the reader is referred to the Web version of this article.)

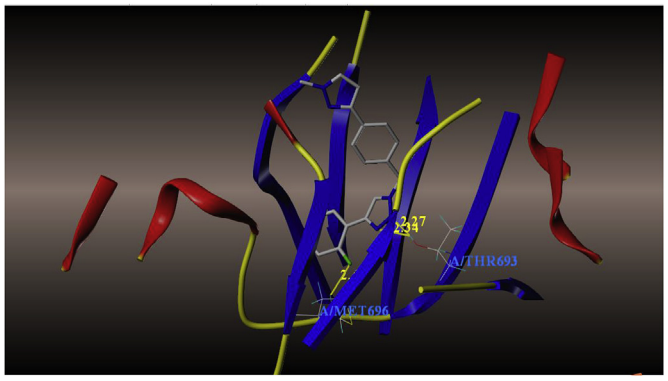

Fig. 4. Superimposition of the docking poses for EphB4 (PDB ID: 4BB4) with compound (7e) and native ligand (cyan). Hydrogen bonds were depicted in dashed yellow lines. (For interpretation of the references to colour in this figure legend, the reader is referred to the Web version of this article.)

3. Conclusion

Acquired resistance caused by compensatory activation of RTKs limits the benefit of anti-angiogenic drugs. It has been revealed that combinatorial inhibiting of multiple pro-angiogenic factors could suppress angiogenesis more efficiently than single-target inhibition. Herein, we described the design, synthesis, and evaluation of novel multi-target inhibitors of VEGFR-2/Tie-2/EphB4 as anti-angiogenic agents.

The results suggested that most of them were potent against those three RTKs. Compounds **6a, 6d**, and **7e** displayed high inhibitory activity against VEGFR-2/Tie-2/EphB4. Anti-proliferation assay indicated that most of the title compounds exhibited potent inhibitory activity against EA.hy926. Among them, compounds **6a, 6d**, and **7e** displayed potent growth inhibition on HUVECs. Structure-activity relationship study suggested that the triazole moiety played an important role in the anti-angiogenic potency. The results suggested an important and favorable role of the *para*-fluoro and methyl substituents in the inhibition of VEGFR-2, Tie-2, and EphB4. The heterocyclic ring could improve the affinity of the multi-target RTKIs as they could form hydrogen bonds with hinge region of RTKs. Molecular modelling indicated that **7e** formed hydrogen bonds with three RTKs along with high affinity, which could be a candidate for further study. The simultaneous inhibition of angiogenic RTKs could be recognized as valuable strategies to

maximize the therapeutic potential and overcome the resistance. This novel strategy may give promising results in the discovery of anti-angiogenic agents.

4. Experimental section

4.1. Chemistry: general procedure

Reagents and solvents are purified according to the standard procedure. The reactions except those in aqueous are performed by standard techniques for the exclusion of moisture. Reactions are monitored by thin layer chromatography (TLC) on 0.25-mm silica gel plates (60 GF-254) and visualized with UV light. Melting points are determined on electrothermal melting point apparatus and are uncorrected. Nuclear magnetic resonance spectra (^{1}H-NMR and ^{13}C-NMR) were recorded on a Bruker Advance AC 400 instrument with DMSO-d_6 as solvent at 400 MHz and 101 MHz, respectively. Chemical shift (δ) are reported in parts per million (ppm) using tetramethylsilane (TMS) as an internal standard, and coupling constants (*J*) are expressed in hertz (Hz). Multiplicities are shown as the abbreviations: s (singlet), brs (broad singlet), d (doublet), t (triplet), m (multiplet).

4.1.1. General procedure for the synthesis of title compounds 6a-6h

4.1.1.1. 1-(azidomethyl)-4-bromobenzene (3).

1-bromo-4-(bromomethyl)benzene (2.00 g 8.00 mmol) was dissolved in anhydrous DMF on ice-bath, 0.78 g (11.99 mmol) of sodium azide dissolved in water was add onto the mixture. Stirring continued for 10min, 0.78 g (11.99 mmol) of sodium azide dissolved in water was dropwise to above mixture at room temperature. The reaction mixture was stirred at room temperature overnight. Subsequently, the organic solvent phase was washed with water and brine (60 mL×3), and dried over Na_2SO_4. After filtration and concentration *in vacuo*, the residue was purified by silica gel flash chromatography affording **(3)** as a slight yellow oil (1.45 g 85.1%).

4.1.1.2. 1-(4-bromobenzyl)-4-(3-chlorophenyl)-1H-1,2,3-triazole (4).

A flask charged with 1-(azidomethyl)-4-bromobenzene **(3)** (1.20 g 5.63 mmol), 1-chloro-3-ethynylbenzene (0.78 g, 5.63 mmol) was dissolved in anhydrous ethanol (30 ml). *L*-Sodium ascorbate (0.45 g, 2.25 mmol), copper sulfate pentahydrate (0.29 g, 1.13 mmol) and water (3 ml) were then add onto the mixture. The reaction mixture was stirred at room temperature overnight. After filtration and concentration *in vacuo*, the residue was purified by silica gel flash chromatography (PE/AcOEt = 3:1) affording **(4)** as white solid (1.31 g, 66.7%)

4.1.1.3. 5-(4-{[4-(3-chlorophenyl)-1H-1,2,3-triazol-1-yl] methyl} phenyl)pyrimidine (6a).

A flask charged with Pd(dppf)Cl_2 (0.25.g, 0.34 mmol), Cs_2CO_3 (3.57 g, 10.35 mmol), and 1-(4-bromobenzyl)-4-(3-chlorophenyl)-1*H*-1,2,3-triazole **(4)** (1.20 g, 3.44 mmol) and pyrimidin-5-ylboronic acid **(5)** (0.60 g, 4.82 mmol) were flushed with nitrogen and suspended in 1,4-dioxane (30 mL) and water (10 mL). The mixture was then refluxed overnight under nitrogen. The hot suspension was filtered and the filtrate distilled by rotary evaporation to remove 1,4-dioxane. Water (50 mL) was added and the product was extracted with AcOEt (60 mL×3), washed with water, and dried over Na_2SO_4. After filtration and concentration *in vacuo*, the residue was purified by silica gel flash chromatography (PE/AcOEt = 15:1) affording **(6a)** as white solid (0.34 g, 28%). m.p. = 176–178 °C. MS (EI) $[M]^+$: $m/z = 347$. ^{1}H NMR (400 MHz, DMSO-d_6) δ 9.20 (s, 1H), 9.15 (s, 2H), 8.81 (s, 1H), 7.93 (s, 1H), 7.86 (d, $J = 8.0$ Hz, 3H), 7.50 (dd, $J = 23.7$, 7.9 Hz, 3H), 7.40 (d, $J = 8.0$ Hz, 1H), 5.75 (s, 2H). ^{13}C NMR (101 MHz, DMSO) δ 157.92, 155.28, 145.90, 137.06, 134.22, 133.23, 133.20, 131.39, 129.44, 128.21, 127.94, 125.29, 124.18, 122.94, 53.24.

The title compounds **6b-6g** were prepared by using the General Procedure described above.

4.1.1.4. 5-(4-{[4-(2-fluorophenyl)-1H-1,2,3-triazol-1-yl]methyl} phenyl)pyrimidine (6b).

m.p. = 152–154 °C, MS (EI) $[M]^+$: $m/z = 345$. ^{1}H NMR (400 MHz, DMSO-d_6) δ 9.20 (s, 1H), 9.14 (s, 2H), 8.62 (d, $J = 3.8$ Hz, 1H), 8.18–8.11 (m, 1H), 7.85 (d, $J = 8.3$ Hz, 2H), 7.57–7.52 (m, 2H), 7.45–7.38 (m, 1H), 7.38–7.30 (m, 2H), 5.78 (s, 2H). ^{13}C NMR (101 MHz, DMSO) δ 157.88, 155.26, 137.26, 134.13, 133.20, 130.26, 130.17, 129.37, 127.90, 127.81, 127.77, 125.49, 125.46, 124.63, 124.51, 118.83, 118.70, 116.63, 116.41, 53.01.

4.1.1.5. 5-{4-[(4-phenyl-1H-1,2,3-triazol-1-yl)methyl]phenyl} pyrimidine (6c).

m.p. = 147–149 °C, MS (EI) $[M]^+$: $m/z = 313$. ^{1}H NMR (400 MHz, DMSO-d_6) δ 9.20 (s, 1H), 9.15 (s, 2H), 8.71 (s, 1H), 7.86 (dd, $J = 7.7$, 3.3 Hz, 4H), 7.53 (d, $J = 8.2$ Hz, 2H), 7.45 (t, $J = 7.6$ Hz, 2H), 7.34 (t, $J = 7.4$ Hz, 1H), 5.74 (s, 2H). ^{13}C NMR (101 MHz, DMSO) δ 157.91, 155.27, 147.24, 137.27, 134.16, 133.22, 131.14, 129.42, 129.35, 128.44, 127.93, 125.68, 122.17, 53.13.

4.1.1.6. 5-(4-{[4-(4-methylphenyl)-1H-1,2,3-triazol-1-yl]methyl} phenyl)pyrimidine (6d).

m.p. = 203–205 °C, MS (EI) $[M]^+$: $m/z = 327$. ^{1}H NMR (400 MHz, DMSO-d_6) δ 9.20 (s, 1H), 9.15 (s, 2H), 8.64 (s, 1H), 7.85 (d, $J = 8.3$ Hz, 2H), 7.75 (d, $J = 8.1$ Hz, 2H), 7.52 (d, $J = 8.2$ Hz, 2H), 7.26 (d, $J = 8.0$ Hz, 2H), 5.72 (s, 2H), 2.33 (s, 3H).^{13}C NMR (101 MHz, DMSO) δ 157.92, 155.28, 147.30, 137.74, 137.30, 134.15, 133.23, 129.97, 129.37, 128.38, 127.93, 125.62, 121.73, 53.10, 21.34.

4.1.1.7. 5-(4-{[4-(3-methylphenyl)-1H-1,2,3-triazol-1-yl]methyl} phenyl)pyrimidine (6e).

m.p. = 165–167 °C, MS (EI) $[M]^+$: $m/z = 327$. ^{1}H NMR (400 MHz, DMSO-d_6) δ 9.20 (s, 1H), 9.15 (s, 2H), 8.68 (s, 1H), 7.89–7.83 (m, 2H), 7.73–7.61 (m, 2H), 7.55–7.51 (m, 2H), 7.33 (t, $J = 7.6$ Hz, 1H), 7.15 (d, $J = 7.5$ Hz, 1H), 5.73 (s, 2H), 2.36 (s, 3H).^{13}C NMR (101 MHz, DMSO) δ 157.92, 155.28, 147.34, 138.57, 137.27, 134.17, 133.22, 131.05, 129.38, 129.32, 129.08, 127.93, 126.25, 122.84, 122.10, 53.13, 21.55.

4.1.1.8. 5-[4-({4-[4-(trifluoromethyl)phenyl]-1H-1,2,3-triazol-1-yl} methyl)phenyl]pyrimidine (6f).

m.p. = 194–196 °C, MS (EI) $[M]^+$: $m/z = 381$. ^{1}H NMR (400 MHz, DMSO-d_6) δ 9.20 (s, 1H), 9.15 (s, 2H), 8.89 (s, 1H), 8.10 (d, $J = 8.1$ Hz, 2H), 7.84 (dd, $J = 16.1$, 8.3 Hz, 4H), 7.55 (d, $J = 8.2$ Hz, 2H), 5.77 (s, 2H). ^{13}C NMR (101 MHz, DMSO) δ 157.93, 155.28, 145.86, 137.05, 135.10, 134.25, 133.20, 129.45, 127.96, 126.44, 126.40, 126.22, 123.46, 123.40, 53.26.

4.1.1.9. 3-[1-(4-pyrimidin-5-ylbenzyl)-1H-1,2,3-triazol-4-yl]aniline (6g).

m.p. = 180–182 °C, MS (EI) $[M]^+$: $m/z = 328$. ^{1}H NMR (400 MHz, DMSO-d_6) δ 9.20 (s, 1H), 9.15 (s, 2H), 8.53 (s, 1H), 7.85 (d, $J = 8.3$ Hz, 2H), 7.52 (d, $J = 8.3$ Hz, 2H), 7.08 (dd, $J = 16.2$, 8.5 Hz, 2H), 6.94 (d, $J = 7.7$ Hz, 1H), 6.53 (d, $J = 8.7$ Hz, 1H), 5.71 (s, 2H), 5.19 (s, 2H). ^{13}C NMR (101 MHz, DMSO) δ 157.91, 155.28, 149.58, 147.91, 137.38, 134.13, 133.24, 131.58, 129.88, 129.35, 127.91, 121.70, 114.14, 113.52, 110.95, 53.03.

4.1.1.10. N-{3-[1-(4-pyrimidin-5-ylbenzyl)-1H-1,2,3-triazol-4-yl] phenyl}cyclopropanecarboxamide (6h).

3-(1-(4-(pyrimidin-5-yl)benzyl)-1H-1,2,3-triazol-4-yl) aniline **(6g)** (0.20 g, 0.60 mmol) was dissolved in anhydrous CH_2Cl_2 (10 mL) and the mixture was stirred on the ice-bath. Triethanolamine (0.15 mL, 1.08 mmol) diluted with CH_2Cl_2 (2 mL) was then added onto the mixture. Stirring was continued for 30 min, a solution of cyclopropanecarbonyl chloride (0.12 mL, 1.20 mmol) in anhydrous CH_2Cl_2 was added dropwise to the above mixture. Then, the ice

bath was removed, and the mixture was reacted at room temperature overnight. The product was extracted with CH_2Cl_2 (30 mL × 3), washed twice with water and brine, and dried over Na_2SO_4. After filtration and concentration *in vacuo*, the residues was purified by silica gel flash chromatography (PE/ AcOEt = 15:1) afford (6h) as white solid (0.20 g, 83%). m.p. = 210–212 °C, MS (EI) $[M]^+$: m/z = 395. ^{1}H NMR (400 MHz, DMSO-d_6) δ 10.32 (s, 1H), 9.20 (s, 1H), 9.15 (s, 2H), 8.65 (s, 1H), 8.17 (t, J = 1.9 Hz, 1H), 7.85 (d, J = 8.3 Hz, 2H), 7.54 (d, J = 8.2 Hz, 3H), 7.48 (d, J = 7.8 Hz, 1H), 7.35 (t, J = 7.9 Hz, 1H), 5.73 (s, 2H), 1.80 (s, 1H), 0.82 (s, 4H). ^{13}C NMR (101 MHz, DMSO) δ 172.29, 157.93, 155.31, 147.20, 140.42, 137.29, 134.20, 133.26, 131.56, 129.87, 129.44, 127.96, 122.18, 120.47, 118.99, 116.12, 53.13, 15.07, 7.75.

4.1.1.11. 4-(2-fluorophenyl)-1-[4-(1H-pyrazol-4-yl)benzyl]-1H-1,2,3-triazole ***(7a)***. A flask charged with Pd(dppf)Cl_2 (0.26 g, 0.36 mmol), CS_2CO_3 (3.52 g, 10.81 mmol), and 1-(4-bromobenzyl)-4-(2-fluorophenyl)-1H-1,2,3-triazole **(4)** (1.20 g 3.60 mmol) and 4-(4,4,5,5-tetramethyl-1,3,2-dioxaborolan-2-yl)-1H-pyrazole **(5)** (0.91 g, 4.68 mmol) were flushed with nitrogen and suspended in 1,4-dioxane (30 mL) and water (10 mL). The mixture was then refluxed overnight under nitrogen. The hot suspension was filtered and the filtrate distilled by rotary evaporation to remove 1,4-dioxane. Water (50 mL) was added and the product was extracted with AcOEt (60 mL×3), washed with water, and dried over Na_2SO_4. After filtration and concentration *in vacuo*, the residue was purified by silica gel flash chromatography (PE/AcOEt = 15:1) affording **(7a)** as white solid (0.20 g, 17%). m.p. = 232–234 °C, MS (EI) $[M]^+$: m/z = 319. ^{1}H NMR (400 MHz, DMSO-d_6) δ 12.97 (s, 1H), 8.55 (d, J = 3.9 Hz, 1H), 8.17 (d, J = 24.9 Hz, 2H), 7.92 (s, 1H), 7.63 (d, J = 8.1 Hz, 2H), 7.36 (dd, J = 17.6, 7.5 Hz, 5H), 5.67 (s, 2H). ^{13}C NMR (101 MHz, DMSO) δ 160.19, 157.74, 140.39, 133.84, 133.45, 129.12, 127.84, 127.80, 125.90, 125.50, 125.46, 124.42, 124.30, 121.11, 118.91, 118.78, 116.64, 116.42, 53.24.

The title compounds **7b-7k** were prepared by using the General Procedure described above.

4.1.1.12. 4-(3-methylphenyl)-1-[4-(1H-pyrazol-4-yl)benzyl]-1H-1,2,3-triazole ***(7b)***. m.p. = 190–192 °C, MS (EI) $[M]^+$: m/z = 315. ^{1}H NMR (400 MHz, DMSO-d_6) δ 12.97 (s, 1H), 8.61 (s, 1H), 8.20 (s, 1H), 7.93 (s, 1H), 7.75–7.57 (m, 4H), 7.34 (dd, J = 18.9, 7.8 Hz, 3H), 7.14 (d, J = 7.3 Hz, 1H), 5.61 (s, 2H), 2.35 (s, 3H). ^{13}C NMR (101 MHz, DMSO) δ 147.25, 138.54, 136.79, 133.80, 133.45, 131.11, 129.30, 129.11, 129.03, 126.23, 125.91, 122.81, 121.87, 121.11, 53.35, 21.54.

4.1.1.13. 1-[4-(1H-pyrazol-4-yl)benzyl]-4-[4-(trifluoromethyl) phenyl]-1H-1,2,3-triazole ***(7c)***. m.p. = 282–284 °C, MS (EI) $[M]^+$: m/z = 369. ^{11}H NMR (400 MHz, DMSO-d_6) δ 12.98 (s, 1H), 8.83 (s, 1H), 8.21 (s, 1H), 8.09 (d, J = 8.1 Hz, 2H), 7.93 (s, 1H), 7.81 (d, J = 8.3 Hz, 2H), 7.64 (d, J = 8.2 Hz, 2H), 7.37 (d, J = 8.2 Hz, 2H), 5.65 (s, 2H).^{13}C NMR (101 MHz, DMSO) δ 145.79, 135.16, 133.58, 129.18, 128.65, 128.34, 126.42, 126.39, 126.19, 125.94, 123.41, 123.23, 121.10, 53.49.

4.1.1.14. 3-{1-[4-(1H-pyrazol-4-yl)benzyl]-1H-1,2,3-triazol-4-yl}aniline ***(7d)***. m.p. = 233–235 °C, MS (EI) $[M]^+$: m/z = 316. ^{1}H NMR (400 MHz, DMSO-d_6) δ 12.99 (s, 1H), 8.48 (s, 1H), 8.22 (s, 1H), 7.94 (s, 1H), 7.64 (d, J = 8.3 Hz, 2H), 7.37 (d, J = 8.2 Hz, 2H), 7.08 (dd, J = 16.1, 8.4 Hz, 2H), 6.95 (d, J = 7.6 Hz, 1H), 6.53 (d, J = 7.9 Hz, 1H), 5.61 (s, 2H), 5.19 (s, 2H).^{13}C NMR (101 MHz, DMSO) δ 149.52, 147.78, 133.89, 133.37, 131.60, 129.82, 129.05, 126.11, 125.86, 121.44, 121.09, 114.05, 113.46, 110.89, 53.22.

4.1.1.15. 4-(2-fluorophenyl)-1-[4-(1-methyl-1H-pyrazol-4-yl) benzyl]-1H-1,2,3-triazole ***(7e)***. m.p. = 147–149 °C, MS (EI) $[M]^+$: m/z = 333. ^{1}H NMR (400 MHz, DMSO-d_6) δ 8.55 (d, J = 3.8 Hz, 1H), 8.16–8.11 (m, 2H), 7.86 (s, 1H), 7.58 (d, J = 8.2 Hz, 2H), 7.41 (d, J = 7.0 Hz, 1H), 7.37 (d, J = 8.3 Hz, 2H), 7.35–7.30 (m, 2H), 5.67 (s, 2H), 3.85 (s, 3H). ^{13}C NMR (101 MHz, DMSO) δ 160.19, 157.74, 140.42, 140.39, 136.61, 133.96, 133.13, 130.22, 130.14, 129.15, 128.44, 127.83, 127.80, 125.71, 125.49, 125.46, 124.44, 124.33, 121.82, 118.91, 118.78, 116.63, 116.42, 53.21, 39.16.

4.1.1.16. 1-[4-(1-methyl-1H-pyrazol-4-yl)benzyl]-4-phenyl-1H-1,2,3-triazole ***(7f)***. m.p. = 195–197 °C, MS (EI) $[M]^+$: m/z = 315.^{1}H NMR (400 MHz, DMSO-d_6) δ 8.65 (s, 1H), 8.14 (s, 1H), 7.88–7.83 (m, 3H), 7.58 (d, J = 8.2 Hz, 2H), 7.44 (t, J = 7.6 Hz, 2H), 7.39–7.31 (m, 3H), 5.62 (s, 2H), 3.86 (s, 3H).^{13}C NMR (101 MHz, DMSO) δ 147.16, 136.61, 133.93, 133.13, 131.19, 129.41, 129.11, 128.45, 128.40, 125.73, 125.66, 121.98, 121.83, 53.33, 39.17.

4.1.1.17. 4-(4-methylphenyl)-1-[4-(1-methyl-1H-pyrazol-4-yl) benzyl]-1H-1,2,3-triazole ***(7g)***. m.p. = 213–215 °C, MS (EI) $[M]^+$: m/z = 329. ^{1}H NMR (400 MHz, DMSO-d_6) δ 8.59 (s, 1H), 8.14 (s, 1H), 7.86 (s, 1H), 7.74 (d, J = 8.1 Hz, 2H), 7.58 (d, J = 8.2 Hz, 2H), 7.35 (d, J = 8.2 Hz, 2H), 7.25 (d, J = 8.0 Hz, 2H), 5.61 (s, 2H), 3.86 (s, 3H), 2.32 (s, 3H). ^{13}C NMR (101 MHz, DMSO) δ 153.85, 147.24, 137.69, 136.62, 133.97, 133.12, 129.96, 129.13, 128.46, 125.73, 125.60, 121.83, 121.55, 53.30, 39.17, 21.34.

4.1.1.18. 4-(3-methylphenyl)-1-[4-(1-methyl-1H-pyrazol-4-yl) benzyl]-1H-1,2,3-triazole ***(7h)***. m.p. = 194–196 °C, MS (EI) $[M]^+$: m/z = 329. ^{1}H NMR (400 MHz, DMSO-d_6) δ 8.62 (s, 1H), 8.14 (s, 1H), 7.86 (s, 1H), 7.69 (s, 1H), 7.64 (d, J = 7.8 Hz, 1H), 7.58 (d, J = 8.2 Hz, 2H), 7.33 (dd, J = 17.1, 8.0 Hz, 3H), 7.14 (d, J = 7.5 Hz, 1H), 5.61 (s, 2H), 3.85 (s, 3H), 2.35 (s, 3H). ^{13}C NMR (101 MHz, DMSO) δ 147.26, 138.56, 136.62, 133.93, 133.14, 131.10, 129.32, 129.15, 129.05, 128.46, 126.24, 125.73, 122.82, 121.91, 121.84, 53.34, 40.00, 39.18, 21.55.

4.1.1.19. 1-[4-(1-methyl-1H-pyrazol-4-yl)benzyl]-4-[4-(trifluoromethyl)phenyl]-1H-1,2,3-triazole ***(7i)***. m.p. = 197–199 °C, MS (EI) $[M]^+$: m/z = 383. ^{1}H NMR (400 MHz, DMSO-d_6) δ 8.83 (s, 1H), 8.14 (s, 1H), 8.09 (d, J = 8.1 Hz, 2H), 7.87 (s, 1H), 7.81 (d, J = 8.3 Hz, 2H), 7.59 (d, J = 8.2 Hz, 2H), 7.37 (d, J = 8.3 Hz, 2H), 5.66 (s, 2H), 3.86 (s, 3H). ^{13}C NMR (101 MHz, DMSO) δ 145.80, 136.62, 135.16, 133.70, 133.22, 129.21, 128.46, 126.42, 126.38, 126.19, 125.76, 123.41, 123.26, 121.82, 53.47, 39.16.

4.1.1.20. 1-[4-(1-methyl-1H-pyrazol-4-yl)benzyl]-4-[3-(trifluoromethyl)phenyl]-1H-1,2,3-triazole ***(7j)***. m.p. = 136–138 °C, MS (EI) $[M]^+$: m/z = 383. ^{1}H NMR (400 MHz, DMSO-d_6) δ 8.85 (s, 1H), 8.17 (d, J = 20.1 Hz, 3H), 7.87 (s, 1H), 7.70 (d, J = 5.1 Hz, 2H), 7.59 (d, J = 8.2 Hz, 2H), 7.37 (d, J = 8.2 Hz, 2H), 5.65 (s, 2H), 3.86 (s, 3H). ^{13}C NMR (101 MHz, DMSO) δ 145.80, 136.62, 133.68, 133.22, 132.26, 130.62, 129.44, 129.23, 128.46, 126.01, 125.76, 124.88, 124.84, 123.30, 122.96, 122.03, 121.99, 121.82, 53.50, 39.16.

4.1.1.21. 3-{1-[4-(1-methyl-1H-pyrazol-4-yl)benzyl]-1H-1,2,3-triazol-4-yl}aniline ***(7k)***. m.p. = 194–196 °C, MS (EI) $[M]^+$: m/z = 330. ^{1}H NMR (400 MHz, DMSO-d_6) δ 12.98 (s, 1H), 8.46 (s, 1H), 8.20 (s, 1H), 7.93 (s, 1H), 7.63 (d, J = 8.2 Hz, 2H), 7.35 (d, J = 8.2 Hz, 2H), 7.07 (dd, J = 16.1, 8.4 Hz, 2H), 6.93 (d, J = 7.6 Hz, 1H), 6.52 (d, J = 9.3 Hz, 1H), 5.59 (s, 2H), 5.18 (s, 2H). ^{13}C NMR (101 MHz, DMSO) δ 149.56, 147.83, 136.60, 133.04, 133.08, 131.63, 129.85, 129.11, 128.44, 125.70, 121.84, 121.50, 114.09, 113.51, 110.93, 53.23, 39.16.

4.1.1.22. N-(3-{1-[4-(1-methyl-1H-pyrazol-4-yl)benzyl]-1H-1,2,3-triazol-4-yl}phenyl)cyclopropanecarboxamide ***(7l)***.

3-(1-(4-(1-methyl-1H-pyrazol-4-yl)benzyl)-1H-1,2,3-triazol-4-yl) aniline **(7k)** (0.20 g, 0.61 mmol) was dissolved in anhydrous CH_2Cl_2 (10 mL) and the mixture was stirred on the ice-bath.

Triethanolamine (0.15 mL, 1.09 mmol) diluted with CH_2Cl_2 (2 mL) was then added onto the mixture. Stirring was continued for 30 min, a solution of cyclopropanecarbonyl chloride (0.12 mL, 1.22 mmol) in anhydrous CH_2Cl_2 was added dropwise to the above mixture. Then, the ice bath was removed, and the mixture was reacted at room temperature overnight. The product was extracted with CH_2Cl_2 (30 mL × 3), washed twice with water and brine, and dried over Na_2SO_4. After filtration and concentration *in vacuo*, the residues was purified by silica gel flash chromatography (PE/AcOEt = 15:1) afford **(7l)** as white solid (0.18 g, 75%). m.p. = 228–230 °C, MS (EI) $[M]^+$: $m/z = 398$. ^{1}H NMR (400 MHz, DMSO-d_6) δ 10.32 (s, 1H), 8.61 (s, 1H), 8.16 (d, J = 5.4 Hz, 2H), 7.87 (s, 1H), 7.58 (t, J = 9.4 Hz, 3H), 7.48 (d, J = 7.7 Hz, 1H), 7.41–7.32 (m, 3H), 5.62 (s, 2H), 3.86 (s, 3H), 1.81 (s, 1H), 0.83 (s, 4H). ^{13}C NMR (101 MHz, DMSO) δ 172.27, 147.10, 140.40, 136.62, 133.94, 133.14, 131.61, 129.84, 129.19, 128.47, 125.73, 121.98, 121.84, 120.45, 118.93, 116.07, 53.32, 39.18, 15.07, 7.74.

4.2. In vitro angiogenic RTKs inhibition assays [24].

The *in vitro* kinase inhibition assays against VEGFR-2, TIE-2, and EphB4 of all the title compounds were detected using the ADP-Glo™ kinase assay kit (Promega, Madison) with Sorafenib as positive control. The kinase assay was performed in a reaction mixture of final volume of 10 μL. General procedures are as the following: for VEGFR-2 assays, the tyrosine kinase (0.6 ng/mL)were incubated with substrates (0.2 mg/mL), test title compounds (1.2×10^{-4}~12 μM) and ATP (50 μM) in a final buffer of Tris 40 mM, $MgCl_2$ 10 mM, BSA 0.1 mg/mL, DTT 1 mM in 384-well plate with the total volume of 5 μL. The assay plate was incubated at 30 °C for 1 h. After the plate was cooled at room temperature for 5 min, 5 μL of ADP-Glo reagent was added into each well to stop the reaction and consume the remaining ADP within 40 min. At the end, 10 μL of kinase detection reagent was added into the well and incubated for 30 min to produce a luminescence signal. As for TIE-2 and EphB4 assays, the tyrosine kinase (2.4 ng/mL)were incubated with substrates (0.2 mg/mL), tested title compounds (1.2×10^{-4}~12 μM) and ATP (50 μM) in a final buffer of Tris 40 mM, $MgCl_2$ 10 mM, BSA 0.1 mg/mL, DTT 1 mM in 384-well plate with the total volume of 5 μL. The assay plate was incubated at 30 °C for 4 h. After the plate was cooled at room temperature for 5 min, 5 μL of ADP-Glo reagent was added into each well to stop the reaction and consume the remaining ADP within 1 h. At the end, 10 μL of kinase detection reagent was added into the well and incubated for 30 min to produce a luminescence signal. The luminescence was read by VICTOR-X multi-label plate reader. The signal was correlated with the amount of ATP present in the reaction and was inversely correlated with the kinase activity.

4.3. Human vascular endothelial cell (EA.hy926) viability assay [25]

The viability of HUVEC (EA.hy926) was assessed using the cell counting kit-8 (CCK-8, Sigma, USA)assay according to the manufacturer's instruction. In brief, EA-hy926 cells were harvested and plated in a 96-wellplate at the density of 1×10^5 cells for each well and cultured in DMEM containing 10% FBS in humidified 5% CO_2 atmosphere. After incubation at 37 °C for 48 h, the cells were treated with tested compounds at various concentrations for 24 h. Subsequently, premixed CCK-8 and medium (10 μL) were added into the 96-well plates to monitor cell viability and were incubated at 37 °C for 2 h. The number of viable cells was assessed by measurement of absorbance at 450 nm by a microplate reader. The viability rate was calculated as experimental OD value/control OD value.

4.4. Anti-proliferative activity against cancer cell lines [26]

Anti-proliferative activities of **7e** were evaluated against fifteen cancer cell lines using 3-(4,5-dimethylthiazol-2-yl)-2,5-diphenyltetrazolium bromide (MTT) method. Exponentially growing cells were harvested and plated in 96-well plates at a concentration of 1×10^4 cells/well per well, and then were incubated at 37 °C for 24 h. The cells were treated with 7e at various concentrations for 48 h. Subsequently, 22 μL fresh MTT (5 mg/mL) was added to each well and incubated at 37 °C for 4 h. 150 mL DMSO was added to each well after supernatant was discarded. Absorbance values were determined by a microplate reader (Bio-Rad Instruments) at 490 nm. The IC_{50} values were calculated according to inhibition ratios.

4.5. Molecular docking modeling [27].

In order to understand the binding mode of inhibitors with VEGFR-2/Tie-2/EphB4, molecule docking was performed using Sybyl-X/Surflex-dock module based on the crystal structures of VEGFR-2 (PDB ID: 4ASD), Tie-2 (PDB ID: 4X3J) and EphB4 (PDB ID: 4BB4). Hydrogen was added and minimized using the Tripos force field and Pullman charges. The most potent compound **7e** was depicted with the Sybyl-X/Sketch module (Tripos Inc.) and optimized applying Powell's method with the Tripos force field with convergence criterion set at 0.05 kcal/(Åmol), and assigned with the Gasteiger-Hückel charge. The docking studied was carried out using Surflex-dock module. The residues in a radius 5.0 Å around the ligand of VEGFR-2/TIE-2/ EphB4 in the crystal complex were selected as the active site. Other docking parameters were kept at default.

Acknowledgments

This work was supported by the National Natural Science Foundation of China (*NSFC*, Grant No. 81573285), the Natural Science Basic Research Plan in Shaanxi Province of China (Program No. 2018JM7071), the Fundamental Research Funds for the Central Universities (2015qngz13), and Hubei Province health and family planning scientific research project (WJ2019M054).

Appendix A. Supplementary data

Supplementary data to this article can be found online at https://doi.org/10.1016/j.ejmech.2018.12.067.

References

[1] Y. Shan, B. Wang, J. Zhang, New strategies in achieving antiangiogenic effect: multiplex inhibitors suppressing compensatory activations of RTKs, Med. Res. Rev. 38 (2018) 1674–1705.
[2] J. Wang, L. Zhang, X. Pan, B. Dai, Y. Sun, C. Li, J. Zhang, Discovery of multi-target receptor tyrosine kinase inhibitors as novel anti-angiogenesis agents, Sci. Rep. 7 (2017) 45145.
[3] J.O. Moore, M.A. Lemmon, K.M. Ferguson, Dimerization of Tie2 mediated by its membrane-proximal FNIII domains, Proc. Natl. Acad. Sci. U. S. A. 114 (2017) 4382–4387.
[4] R. Salgia, P. Kulkarni, P.S. Gill, EphB4: a promising target for upper aero-digestive malignancies, Biochim. Biophys. Acta 1869 (2018) 128–137.
[5] Y. Shan, B. Wang, J. Zhang, New strategies in achieving antiangiogenic effect: multiplex inhibitors suppressing compensatory activations of RTKs, Med. Res. Rev. 38 (2018) 1674–1705.
[6] Z. Lin, Q. Zhang, W. Luo, Angiogenesis inhibitors as therapeutic agents in cancer: challenges and future directions, Eur. J. Pharmacol. 793 (2016) 76–81.
[7] Y. Sun, Y. Shan, C. Li, R. Si, X. Pan, B. Wang, J. Zhang, Discovery of novel anti-angiogenesis agents. Part 8: diaryl thiourea bearing 1H-indazole-3-amine as multi-target RTKs inhibitors, Eur. J. Med. Chem. 141 (2017) 373–385.
[8] C. Li, Y. Shan, Y. Sun, R. Si, L. Liang, X. Pan, B. Wang, J. Zhang, Discovery of novel anti-angiogenesis agents. Part 7: multitarget inhibitors of VEGFR-2, TIE-2 and EphB4, Eur. J. Med. Chem. 141 (2017) 506–518.

[9] W. Chen, G. Zhang, L. Guo, W. Fan, Q. Ma, X. Zhang, R. Du, R. Cao, Synthesis and biological evaluation of novel alkyl diamine linked bivalent β-carbolines as angiogenesis inhibitors, Eur. J. Med. Chem. 124 (2016) 249–261.
[10] M.A. Abdullaziz, H.T. Abdel-Mohsen, A.M. El Kerdawy, F.A.F. Ragab, M.M. Ali, S.M. Abu-Bakr, A.S. Girgis, H.I. El Diwani, Design, synthesis, molecular docking and cytotoxic evaluation of novel 2-furybenzimidazoles as VEGFR-2 inhibitors, Eur. J. Med. Chem. 136 (2017) 315–329.
[11] P.K. Parikh, M.D. Ghate, Recent advances in the discovery of small molecule c-Met Kinase inhibitors, Eur. J. Med. Chem. 143 (2018) 1103–1138.
[12] M. Wei, X. Peng, L. Xing, Y. Dai, R. Huang, M. Geng, A. Zhang, J. Ai, Z. Song, Design, synthesis and biological evaluation of a series of novel 2-benzamide-4-(6-oxy-*N*-methyl-1-naphthamide)-pyridine derivatives as potent fibroblast growth factor receptor (FGFR) inhibitors, Eur. J. Med. Chem. 154 (2018) 9–28.
[13] H. Zhang, X. Fang, Q. Meng, Y. Mao, Y. Xu, T. Fan, J. An, Z. Huang, Design, synthesis and characterization of potent microtubule inhibitors with dual anti-proliferative and anti-angiogenic activities, Eur. J. Med. Chem. 157 (2018) 380–396.
[14] L. Zhang, Y. Shan, X. Ji, M. Zhu, C. Li, Y. Sun, R. Si, X. Pan, J. Wang, W. Ma, Dai, B. Wang, J. Zhang, Discovery and evaluation of triple inhibitors of VEGFR-2, TIE-2 and EphB4 as anti-angiogenic and anti-cancer agents, Oncotarget 8 (2017) 104745–104760.
[15] L. Chavez-Acevedo, L.D. Miranda, Synthesis of novel tryptamine-based macrocycles using an Ugi 4-CR/microwave assisted click-cycloaddition reaction protocol, Org. Biomol. Chem. 13 (2015) 4408–4412.
[16] N. Vohradská, E.M. Sánchez-Carnerero, T. Pastierik, C. Mazal, P. Klán, Controlled photorelease of alkynoic acids and their decarboxylative deprotection for copper-catalyzed azide/alkyne cycloaddition, Chem. Commun. (Camb). 54 (2018) 5558–5561.
[17] L. Zhang, Y. Shan, C. Li, Y. Sun, P. Su, J. Wang, L. Li, X. Pan, J. Zhang, Discovery of novel anti-angiogenesis agents. Part 6: multi-targeted RTK inhibitors, Eur. J. Med. Chem. 127 (2017) 275–285.
[18] S. Zheng, Q. Zhong, M. Mottamal, Q. Zhang, C. Zhang, E. Lemelle, H. McFerrin, G. Wang, Design, synthesis, and biological evaluation of novel pyridine-bridged analogues of combretastatin-A4 as anticancer agents, J. Med. Chem. 57 (2014) 3369–3381.
[19] M. Vojtičková, J. Dobiaš, G. Hanquet, G. Addová, R. Cetin-Atalay, D.C. Yildirim, A. Boháč, Ynamide Click chemistry in development of triazole VEGFR2 TK modulators, Eur. J. Med. Chem. 103 (2015) 105–122.
[20] H. Gao, P. Su, Y. Shi, X. Shen, Y. Zhang, J. Dong, J. Zhang, Discovery of novel VEGFR-2 inhibitors. Part II: biphenyl urea incorporated with salicylaldoxime, Eur. J. Med. Chem. 90 (2015) 232–240.
[21] X. Pan, J. Dong, Y. Shi, R. Shao, F. Wei, J. Wang, J. Zhang, Discovery of novel Bcr-Abl inhibitors with diacylated piperazine as the flexible linker, Org. Biomol. Chem. 13 (2015) 7050–7066.
[22] P. Su, J. Wang, Y. Shi, X. Pan, R. Shao, J. Zhang, Discovery of biphenyl-aryl ureas as novel VEGFR-2 inhibitors. Part 4: exploration of diverse hinge-binding fragments, Bioorg. Med. Chem. 23 (2015) 3228–3236.
[23] J.R. Güette-Fernández, E. Meléndez, W. Maldonado-Rojas, C. Ortega-Zúñiga, J. Olivero-Verbel, E.I. Parés-Matos, A molecular docking study of the interactions between human transferrin and seven metallocene dichlorides, J. Mol. Graph. Model. 75 (2017) 250–265.
[24] H. Zegzouti, J. Hennek, S.A. Goueli, Using bioluminescent kinase profiling strips to identify kinase inhibitor selectivity and promiscuity, Methods Mol. Biol. 1360 (2016) 59–73.
[25] Y. Bai, W. Wang, G. Sun, M. Zhang, J. Dong, Curcumin inhibits angiogenesis by up-regulation of microRNA-1275 and microRNA-1246: a promising therapy for treatment of corneal neovascularization, Cell Prolif 49 (2016) 751–762.
[26] Y. Shan, H. Gao, X. Shao, J. Wang, X. Pan, J. Zhang, Discovery of novel VEGFR-2 inhibitors. Part 5: exploration of diverse hinge-binding fragments via core-refining approach, Eur. J. Med. Chem. 103 (2015) 80–90.
[27] S.D. Joshi, S.R. Dixit, M.N. Kirankumar, T.M. Aminabhavi, K.V. Raju, R. Narayan, C. Lherbet, K.S. Yang, Synthesis, antimycobacterial screening and ligand-based molecular docking studies on novel pyrrole derivatives bearing pyrazoline, isoxazole and phenyl thiourea moieties, Eur. J. Med. Chem. 107 (2016) 133–152.